IOP Publishing Journal of Physics B: Atomic, Molecular and Optical Physics
J. Phys. B: At. Mol. Opt. Phys. **53** (2020) 055201 (10pp) https://doi.org/10.1088/1361-6455/ab6052

Ionization of biological molecules by multicharged ions using the stoichiometric model

A M P Mendez[1], **C C Montanari and J E Miraglia**

Instituto de Astronomía y Física del Espacio (CONICET–UBA), Buenos Aires, Argentina

E-mail: alemendez@iafe.uba.ar

Received 7 October 2019, revised 2 December 2019
Accepted for publication 10 December 2019
Published 4 February 2020

Abstract

In the present work, we investigate the ionization of molecules of biological interest by the impact of multicharged ions in the intermediate to high energy range. We performed full non-perturbative distorted-wave calculations (CDW) for thirty-six collisional systems composed by six atomic targets: H, C, N, O, F, and S—which are the constituents of most of the DNA and biological molecules—and six charged projectiles (antiprotons, H, He, B, C, and O). On account of the radiation damage caused by secondary electrons, we inspect the energy and angular distributions of the emitted electrons from the atomic targets. We examine seventeen molecules: DNA and RNA bases, DNA backbone, pyrimidines, tetrahydrofuran (THF), and C_nH_n compounds. We show that the simple stoichiometric model (SSM), which approximates the molecular ionization cross sections as a linear combination of the atomic ones, gives reasonably good results for complex molecules. We also inspect the extensively used Toburen scaling of the total ionization cross sections of molecules with the number of weakly bound electrons. Based on the atomic CDW results, we propose new active electron numbers, which leads to a better universal scaling for all the targets and ions studied here in the intermediate to the high energy region. The new scaling describes well the available experimental data for proton impact, including small molecules. We perform full molecular calculations for five nucleobases and test a modified stoichiometric formula based on the Mulliken charge of the composite atoms. The difference introduced by the new stoichiometric formula is less than 3%, which indicates the reliability of the SSM to deal with this type of molecules. The results of the extensive ion-target examination included in the present study allow us to assert that the SSM and the CDW-based scaling will be useful tools in this area.

Keywords: DNA bases, DNA ionization, stoichiometric model, multicharged ions, biological molecules, ionization of molecules

1. Introduction

The damage caused by the impact of multicharged heavy projectiles on biological targets has become a field of interest due to its recent implementation in ion-beam cancer therapy. The effectiveness of the radiation depends on the choice of the ions. In particular, theoretical and experimental studies with different projectiles have concluded that charged carbon ions could be the most suitable ions to be used [1]. Nonetheless, the study of such systems represents a challenge from the theoretical point of view.

The ionization of biological molecules by multicharged ions constitutes the primary damage mechanism. The most widely used method to predict such processes is the first Born approximation. At high energies, this perturbative method warrants the Z^2 laws, where Z is the projectile charge. However, the damage is concentrated in the vicinities of the Bragg peak—at energies of hundreds of keV amu^{-1}—, precisely where the Born approximation starts to fail. Another theoretical issue arises due to the targets themselves; we are

[1] Author to whom any correspondence should be addressed.

dealing with complex molecules, and the description of such targets represents a hard task for *ab initio* calculations.

Different approaches have been proposed to deal with the ionization of molecular targets within the independent atom model. For example, Galassi *et al* [2] obtain molecular cross sections by combining CDW-EIS atomic ones based on the population of the molecular orbitals. More recently, Lüdde *et al* [3, 4] propose a combination of atomic cross sections with geometrical screening corrections.

The objective of this article is to face with two aspects of the ionization of biological molecules; first, we perform more appropriate calculations on the primary damage mechanism, which can replace the Born results. Second, we inspect and test a stoichiometric model to describe the ionization of molecular targets.

To overcome the limitations of first order perturbative approximations, and since the projectiles are multicharged ions, we resort to the continuum distorted wave-eikonal initial state (CDW) [2, 5–7], which includes higher perturbative corrections. Details on the CDW calculation are given in section 2. We start from the premise that the ionization process is the mechanism that deposits the most significant amount of primary energy. Moreover, the residual electrons from the ionization are known to be a source of significant local biological damage [8]. The secondary electrons are included in Monte Carlo simulations, and hence their behavior requires further investigation. In sections 2.1 and 2.2, we calculate the mean energy and angular distributions of the ejected electrons. Surprisingly, we found a substantial dependence on the projectile charge, which is unexpected in the first Born approximation.

In section 3.1, we deal with the molecular structure complexity of the targets by implementing the simplest stoichiometric model (SSM): the molecules are assumed to be composed of isolated independent atoms, and the total cross section by a linear combination of stoichiometric weighted atomic calculations. By implementing the CDW and the SSM, we calculate ionization cross section of several molecules of biological interest, including DNA and RNA molecules, such as adenine, cytosine, guanine, thymine, uracil, tetrahydrofuran (THF), pyrimidine, and DNA backbone, by the impact of antiprotons, H^+, He^{2+}, Be^{4+}, C^{6+}, and O^{8+}. In section 3.2, we test the Toburen scaling rule [9, 10], which states that the ratio between the ionization cross section and the number of weakly bound electrons can be arranged in a narrow universal band in terms of the projectile velocity. We applied this rule to several hydrocarbons and nucleobases and noted that the width of the resulting universal band could be significantly reduced if we consider the number of active electrons in the collision based on the CDW results for the different atoms. The new scaling was then tested theoretically and by comparison with experimental data available.

The approach SSM considers the atoms in the molecule as neutral, which is not correct. In section 3.3, we used the molecular electronic structure code GAMESS [11] to calculate the excess or defect of electron density on the atoms composing the molecules. Then, we modified the SSM to account for the departure from the neutrality of the atoms. We find that the modified SSM for the DNA molecules does not introduce substantial changes in the cross sections.

2. Theory: ionization of atoms

In the present study, we consider six atoms, α = H, C, N, O, P, and S, and six projectiles, antiprotons $\bar{p}$, H^+, He^{2+}, Be^{4+}, C^{6+}, and O^{8+}. Most of the organic molecules are composed of these atoms. Some particular molecules also include halogen atoms such as fluorine and bromine; ionization cross sections of these elements have been previously published [6].

The total ionization cross sections of these atoms σ_α were calculated using the CDW. The initial bound and final continuum radial wave functions were obtained by using the RADIALF code, developed by Salvat and co-workers [12], and a Hartree–Fock potential obtained from the Depurated Inversion Method [13, 14]. We used a few thousand pivot points to solve the Schrödinger equation, depending on the number of oscillations of the continuum state. The radial integration was performed using the cubic spline technique. We expand our final continuum wave function as usual

$$\psi^{-}_{\vec{k}}(\vec{r}) = \sum_{l=0}^{l_{\max}} \sum_{m=-l}^{l} R^{-}_{kl}(r)\, Y_l^m(\hat{r})\, Y_l^{m^*}(\hat{k}). \tag{1}$$

The number of angular momenta considered varied from 8, at very low ejected-electron energies, up to $l_{\max} \sim 30$, for the highest energies considered. The same number of azimuth angles were required to obtain the four-fold differential cross section. The calculation performed does not display prior-post discrepancies at all. Each atomic total cross section was calculated using 35–100 momentum transfer values, 28 fixed electron angles, and around 45 electron energies depending on the projectile impact energy. Further details of the calculation are given in [15].

We display our total CDW ionization cross sections for the six essential elements by the impact of the six projectiles in figure 1. To reduce the resulting 36 magnitudes into a single consistent figure, we considered the fact that in the first Born approximation the ionization cross section scales with the square of the projectile charge, Z^2. The impact energies considered range between 0.1 and 10 MeV amu^{-1}, where the CDW is supposed to hold. In fact, for the highest projectile charges the minimum impact energy where the CDW is expected to be valid could be higher than 100 keV. We also performed similar calculations with the first Born approximation, and we corroborated that it provides quite reliable results only for energies higher than a couple of MeV amu^{-1}. We use the same line color to indicate the projectile charge throughout all the figures of this work: dashed-red, solid-red, blue, magenta, olive and orange for antiprotons, H^+, He^{2+}, Be^{4+}, C^{6+}, and O^{8+}, respectively. Notably, there is no complete tabulation of ionization of atoms by the impact of multicharged ions. We hope that the ones presented in this article will be of help for future works.

Simultaneously, we will be reporting state to state ionization cross sections for the 36 ion-target systems considered in the present work [16]. A great numerical effort was

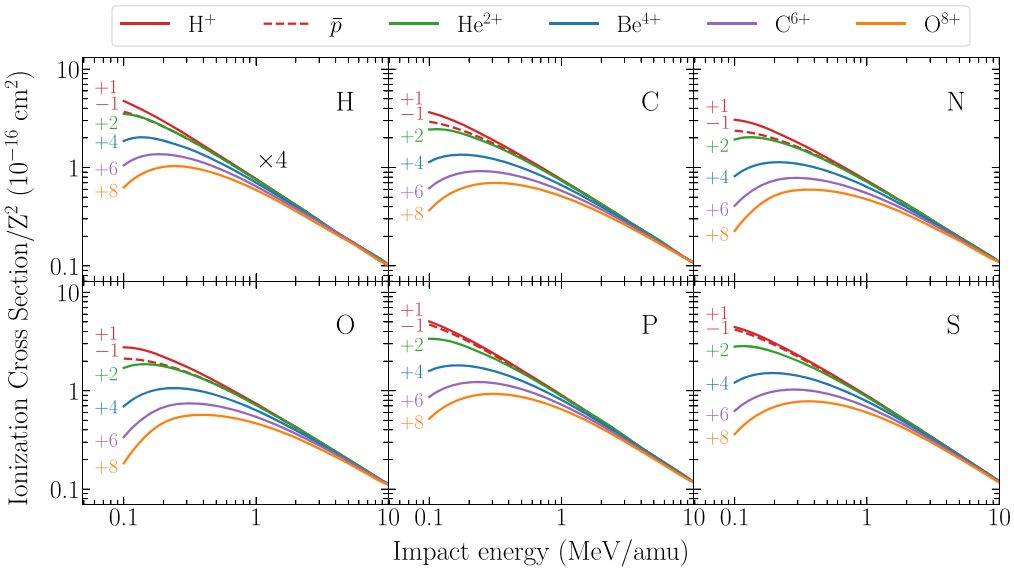

Figure 1. Reduced CDW total ionization cross section σ_α/Z^2 of six atomic targets. The curves are labeled with the charge state corresponding to the six multicharged projectiles.

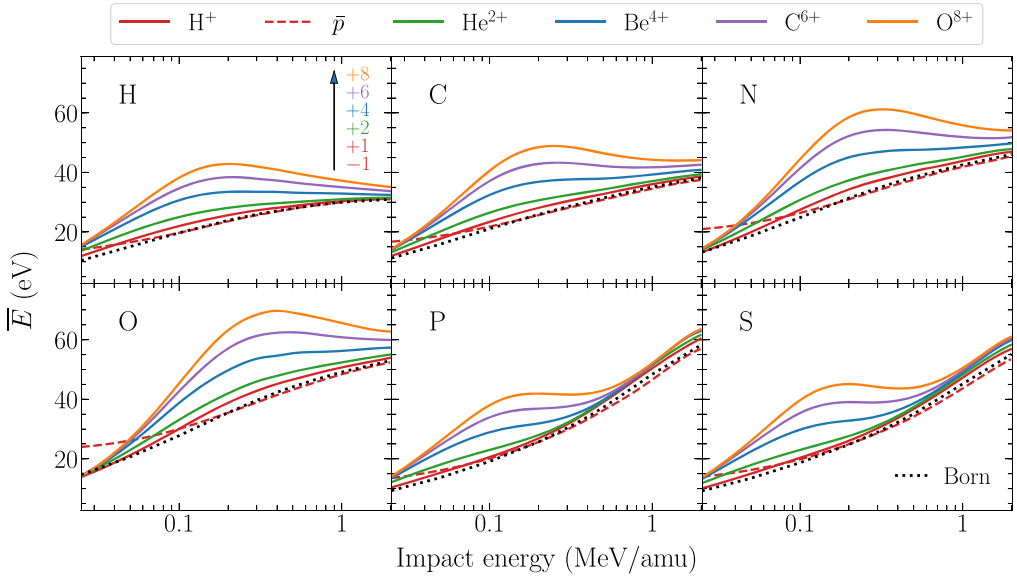

Figure 2. Mean emitted energy distribution for ionization by the impact of multicharged ions, given by equation (2). Solid lines for ion charges +1, 2+, 4+, 6+ and 8+, as indicated. Dashed lines for $\bar{p}$ and dotted line for the Born approximation with $Z = 1$.

paid to obtain these results, and we expect that they will be useful to estimate molecule fragmentation.

2.1. Emitted electron energies

In a given biological medium, direct ionization by ion impact accounts for just a fraction of the overall damage. Secondary electrons, as well as recoil target ions, also contribute substantially to the total damage [8]. We can consider the single differential cross section of the shell nl of the atom α, $d\sigma_{\alpha nl}/dE$, to be a function of the ejected electron energy E as a simple distribution function [17]. Then, we can define the mean value $\overline{E}_\alpha$ as in [18]

$$\overline{E}_\alpha = \frac{\langle E_\alpha \rangle}{\langle 1 \rangle} = \frac{1}{\sigma_\alpha} \sum_{nl} \int dE\, E \frac{d\sigma_{\alpha,nl}}{dE}, \tag{2}$$

$$\langle 1 \rangle = \sigma_\alpha = \sum_{nl} \int dE\, \frac{d\sigma_{\alpha,nl}}{dE}, \tag{3}$$

where Σ_{nl} takes into account the sum of the different sub-shell contributions of the element α.

The mean emitted electron energies $\overline{E}_\alpha$ for H, C, N, O, P and S are shown in figure 2. The range of impact velocities was shortened to $v = 10$ a.u. due to numerical limitations in the spherical harmonics expansion of equation (1). As the impact velocity v increases, so do $\langle E_\alpha \rangle$ and $l_{\max}$, which results in the inclusion of very oscillatory functions in the integrand. Furthermore, the integrand of $\langle E_\alpha \rangle$ includes the kinetic energy E (see equation (2)), which cancels the small energy region and reinforces the large values, making the result more sensible to large angular momenta. Regardless, for $v > 10$ a.u., the first Born approximation holds.

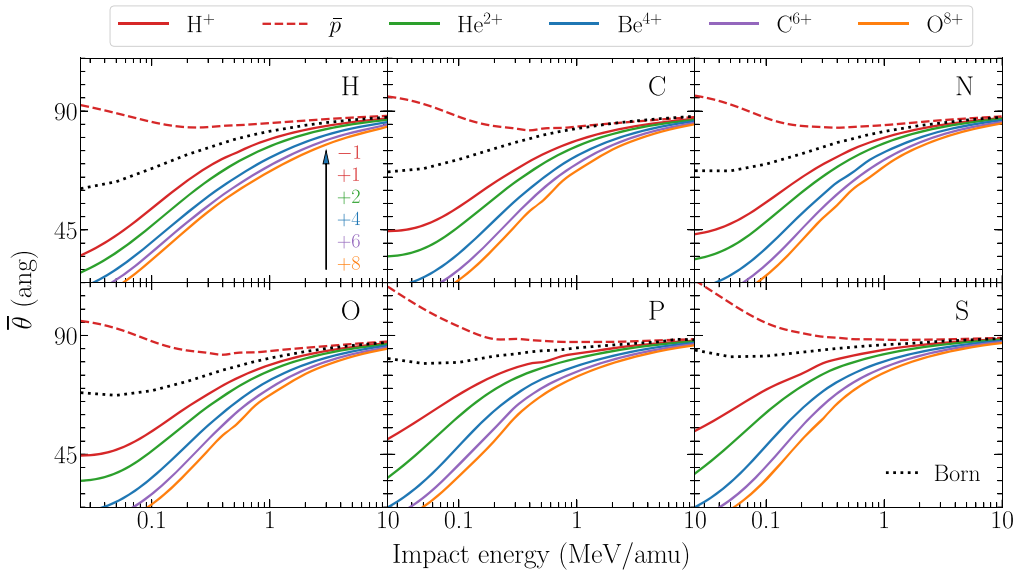

Figure 3. Mean emitted angle distribution for ionization by impact of multicharged ions. Curves as in figure 2.

In figure 2, we estimate $\overline{E}_\alpha$ of the emitted electron in the 10–70 eV energy range, for all the targets. Our results agree with the experimental findings [17]. As can be noted in the figure, the mean energy value is surprisingly sensitive to the projectile charge Z, which can duplicate the proton results in the intermediate region, i.e. 100–400 keV amu^{-1}. The effect observed can be attributed to the depletion caused by the multicharged ions to the yields of low energy electrons. This behavior cannot be found in the first Born approximation, where the Z^2 law cancels the Z dependence in equation (2). At high energies, $\overline{E}_\alpha$ tends to a universal value for all ions, as can be seen in figure 2.

2.2. Emitted electron angles

As mentioned before, secondary electrons contribute to the total damage. Then, not only the ejection energy is essential but also the angle of emission. Once again, we can consider the single differential cross section in terms of the ejected electron solid angle Ω, $d\sigma_{\alpha,nl}/d\Omega$, to be expressed as a distribution function, and the mean angle $\overline{\theta}_\alpha$ can be defined as

$$\overline{\theta}_\alpha = \frac{\langle\theta_\alpha\rangle}{\langle 1\rangle} = \frac{1}{\sigma_\alpha}\sum_{nl}\int d\Omega\,\theta\,\frac{d\sigma_{\alpha,nl}}{d\Omega}, \tag{4}$$

$$\langle 1\rangle = \sigma_\alpha = \sum_{nl}\int d\Omega\,\frac{d\sigma_{\alpha,nl}}{d\Omega}. \tag{5}$$

The mean emitted electron angles $\overline{\theta}_\alpha$ for the six atoms and six ions of interest are shown in figure 3. A significant dependence of $\overline{\theta}_\alpha$ with Z is noticed for all the cases. Once again, this effect could not be observed in the first Born approximation (dotted line).

For low energy electron emission, the angular dispersion is nearly isotropic [19]. A typical value for the ejection angle considered in the literature is $\overline{\theta}_\alpha \sim 70°$ [17], and it is quite correct in the range of validity of the first Born approximation for any target. However, when a distorted wave approximation is used, $\overline{\theta}_\alpha$ decreases substantially with Z in the intermediate energy region, as shown in figure 3. The higher the charge Z, the smaller $\overline{\theta}$ will be. Of course, this effect only holds at intermediate energies and not at high impact energies.

To illustrate this feature, consider the impact of 500 keV C^{6+} on oxygen. The first Born approximation predicts emitted electrons with mean energies of 46.7 eV and mean angles of 78°, while the CDW gives 62.5 eV and 60°. These results imply deeper penetration of the secondary electrons with an orientation closer to the direction of the ion. We can attribute this forward direction correction to the capture to the continuum effect.

Furthermore, figure 3 provides an illustrative description of the behavior of antiprotons: the projectile repels the electrons, being $\overline{\theta}_\alpha \sim 90°$. Note the opposite effect of proton and antiprotons respect to the first Born approximation; this phenomenon constitutes an angular Barkas effect.

3. Ionization of molecules

3.1. The stoichiometric model

Lets us consider a molecule M composed by n_α atoms of the element α, the SSM approaches the total ionization cross section of the molecule σ_M as a sum of ionization cross sections of the isolated atoms σ_α weighted by n_α

$$\sigma_M = \sum_\alpha n_\alpha \sigma_\alpha. \tag{6}$$

We classified the molecular targets of our interest in three families: CH, CHN, and DNA, as in table 1.

In figure 4, we report the reduced total ionization cross sections σ_M/Z^2 for adenine, cytosine, guanine, and thymine by the impact of multicharged ions obtained combining the SSM given by equation (6) and the CDW results. For adenine, the agreement with the experimental data available for proton impact [20] is excellent. To the best of our knowledge, there are no experimental data on ion-collision ionization for the rest of the molecules. We have also included in this figure electron impact measurements [21] with the corresponding

Table 1. Molecular targets studied in this work, classified in three families.

CH	CH_4 (methane), C_2H_2 (acetylene), C_2H_4 (ethene), C_2H_6 (ethane), C_6H_6 (benzene)
CHN	C_5H_5N (pyridine), $C_4H_4N_2$ (pyrimidine), C_2H_7N (dimenthylamine), CH_5N (monomethylamine)
DNA	$C_5H_5N_5$ (adenine), $C_4H_5N_3O$ (cytosine), $C_5H_5N_5O$ (guanine), $C_5H_6N_2O_2$ (thymine), $C_4H_4N_2O_2$ (uracil), C_4H_8O (THF), $C_5H_{10}O_5P$ (DNA backbone), $C_{20}H_{27}N_7O_{13}P_2$ (dry DNA)

equivelocity conversion for electron incident energies higher than 300 eV. In this region, the proton and electron cross section should converge. Although the electron impact measurements are above our findings for all the molecular targets, it is worth stating that our results agree very well with other electron impact theoretical predictions [22, 23].

The reduced total ionization cross sections σ_M/Z^2 for uracil, DNA backbone, pyrimidine, and THF are displayed in figure 5. For uracil, the agreement with the experimental proton impact measurements by Itoh *et al* [24] is good. However, for the same target, our theory is a factor of two above the experimental ionization measurements by Tribedi and collaborators [25, 26] by the impact of multicharged ions. Nonetheless, it should be stated that our theoretical results coincide with calculations by Champion, Rivarola, and collaborators [25, 27], which may indicate a possible misstep of the experiments.

For pyrimidine, we show a comparison of our results with experimental data for proton impact by Wolff [28] and also for electron impact ionization [30] at high energies. The electron impact measurements agree with our calculations for energies higher than 500 keV. Unexpectedly, the proton impact cross sections are significantly lower than our findings. Much more experiments are available for ionization of THF molecule by proton [29] and by electron [30–32] impact. Our SSM with CDW results show overall good agreement with these data.

At intermediate impact energies, the Z^2 rule no longer holds, and other scalings can be considered in this region. For example, the molecular cross section and ion impact energy can be reduced with the projectile charge Z, as suggested in in [33, 34].

3.2. Scaling rules

3.2.1. Toburen rule. The first attempt to develop a comprehensive but straightforward phenomenological model for electron ejection from large molecules was proposed by Toburen and co-workers [9, 10]. The authors found it convenient to scale the experimental ionization cross section in terms of the number of weakly bound electrons, n_e. For instance, for C, N, O, P, and S, this number is the total number of electrons minus the K-shell. Following Toburen, the scaled ionization cross section per weakly bound electron σ_e^T is

$$\sigma_e^T = \frac{\sigma_M}{n_e}, \tag{7}$$

where $n_e = \sum_\alpha n_\alpha \nu_\alpha^T$, and ν_α^T are the Toburen numbers given by

$$\nu_\alpha^T = \begin{cases} 1, & \text{for H,} \\ 4, & \text{for C,} \\ 5, & \text{for N and P,} \\ 6, & \text{for O and S.} \end{cases} \tag{8}$$

The Toburen rule can be stated by saying that σ_e is a *universal* parameter independent on the molecule, which depends solely on the impact velocity, and holds for high impact energies (i.e. 0.25–5 MeV amu^{-1}). These ν_α^T can be interpreted as the number of active electrons in the collision. At very high energies, the K-shell electrons will also be ionized, and these numbers will be different. A similar dependence with the number of weakly bound electrons was found in [24] for proton impact on uracil and adenine.

Following the Toburen scaling, we computed the scaled CDW cross sections σ_e^T for the molecular targets of table 1. Our results are shown in figure 6(a) as a function of the impact energy for different projectile charges. Although the Toburen scaling holds for high energies, its performance is still not satisfactory: the universal band is quite broad, as can be noted in this figure.

3.2.2. CDW-based scaling. The departure of our theoretical results from the Toburen rule can be easily understood by inspecting figure 1. It can be noted that the rule $\sigma_\alpha/\nu_\alpha^T \sim \sigma_e^T$, approximately constant, is not well satisfied by the CDW. For example, figure 1 shows that the cross sections for O are very similar to the cross sections for C, suggesting 4 active electrons in O instead of 6. In the same way, the number of active electrons for N, P, and S obtained with the CDW are also different from the ν_α^T of equation (8).

Based on the CDW results, we propose a new scaling

$$\sigma_e' = \frac{\sigma_M}{n_e'}, \tag{9}$$

where $n_e' = \sum_\alpha n_\alpha \nu_\alpha^{\mathrm{CDW}}$, and $\nu_\alpha^{\mathrm{CDW}}$ are the numbers of active electrons per atom obtained from the CDW ionization cross sections for different ions in H, C, N, O, P, and S targets, given as follows

$$\nu_\alpha^{\mathrm{CDW}} \sim \begin{cases} 1, & \text{for H,} \\ 4, & \text{for C, N, and O,} \\ 4.5, & \text{for P and S.} \end{cases} \tag{10}$$

The new scaled cross sections σ_e' are plotted in figure 6(b). The experimental data for ionization of adenine [20], uracil [24], pyrimidine [28], and THF [29] by proton impact in figure 6(b) seems to corroborate the new scaling. We also included the electron impact ionization measurements with equivelocity

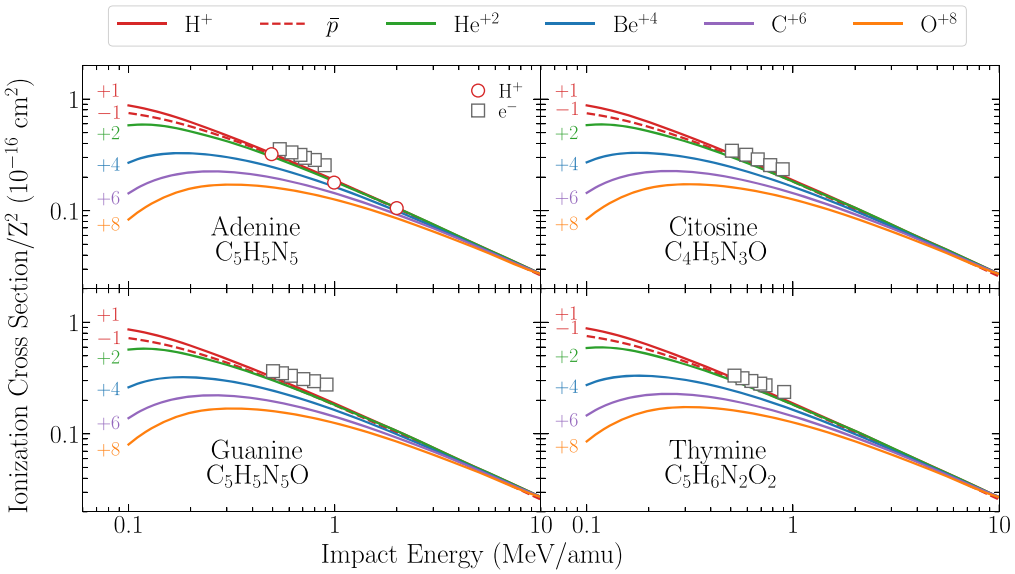

Figure 4. Reduced CDW ionization cross section σ_M/Z^2 as a function of ion impact energy. Experiments: ∘ [20] for proton impact and □ [21] for electron impact with equivelocity conversion.

conversion on pyrimidine [30] and THF [30–32]. It will be interesting to cross-check with future experiments, mainly for higher projectile charge states.

By using equation (10), we define new active electron numbers n_e' for molecules. In table 2, we display the present n_e' values and n_e ones by Toburen obtained from equation (8). Our values are different from the ones proposed by Toburen and used by other authors [24], mainly due to the differences in the active electron numbers of oxygen. An alternative way of testing the present scaling can be attained by plotting the ionization cross sections of molecules as a function of the n_e' from table 2. Our findings are displayed in figure 7 for impact energies 0.5, 1, and 2MeV. As can be noted, the computed CDW ionization cross sections for all the molecules show a linear dependence with the number of electrons n_e' from table 2. We obtain similar results, even for $E = 10$ MeV. The comparison with the experimental data available shows overall good agreement, for the smallest molecules, H_2, H_2O, and CH_4, up to the most complex ones, like adenine. For electron impact data, the experimental data was interpolated between close neighbors. It is worth mentioning that an equivalent plot using the Toburen numbers n_e does not exhibit the straight lines obtained with the present scaling.

While finishing the present work, we became aware of an accepted manuscript by Lüdde *et al* [37] on total ionization of biological molecules by proton impact, using the independent-atom-model pixel counting method [3, 4]. The authors also raised a scaling with $\nu_\alpha = 4$ for C, N, and O, but $\nu_\alpha = 6$ for P. The agreement with this independent method for proton impact reinforces our multicharged-ion findings.

3.3. Molecular structure of targets

Finally, to test the range of validity of the SSM, we performed *ab initio* molecular calculation of five nucleobases by employing the GAMESS code. The geometry optimization and single point energy calculations were performed implementing the restricted Hartree–Fock method and the 3-21G basis set.

The molecular binding energies of the valence electrons for adenine, cytosine, guanine, thymine, and uracil are shown in figure 8. The binding energy of the highest molecular orbital (HOMO) agrees with the experimental values [38–40] within 2% for all the DNA bases considered. On the left side of figure 8, we show the atomic Hartree–Fock energies of the constituent elements, which gives an insight into the distribution of the weakly bound electrons in the molecules. A dashed line around −26 eV is drawn to separate the molecular band in two. We can consider the atomic energy levels above this line as the ones corresponding to the weakly bound electrons from equation (10). For example, the 2*s* and 2*p* electrons of carbon are placed above the separating line, which corresponds to the 4 electrons given by CDW-scaling. In the case of O, only the 4 electrons of the 2*p* orbitals are located above the separating line, which corresponds to the number of weakly bound electron given by our new scaling. The *N* case is not as straightforward; the $\nu_{N=4}^{\mathrm{CDW}}$ would suggest that one out of the two 2*s* electrons contribute to the molecular scheme.

3.3.1. A modified stoichiometric model. The SSM considers the molecule to be assembled by isolated neutral atoms, which is definitively unrealistic. A first improvement can be suggested by assuming that the atoms are not neutral and that they have an uneven distribution of electrons within the molecule, which can be expressed as an effective charge q_α per atom. The Mulliken charge gives a possible value for q_α; however, there are a wide variety of charge distributions [41].

To take this effect into account, we can consider that the total amount of electrons Q_α on the element α is equally distributed on all the α atoms. Therefore, each element α will have an additional charge, $q_\alpha = Q_\alpha/n_\alpha$, which can be positive

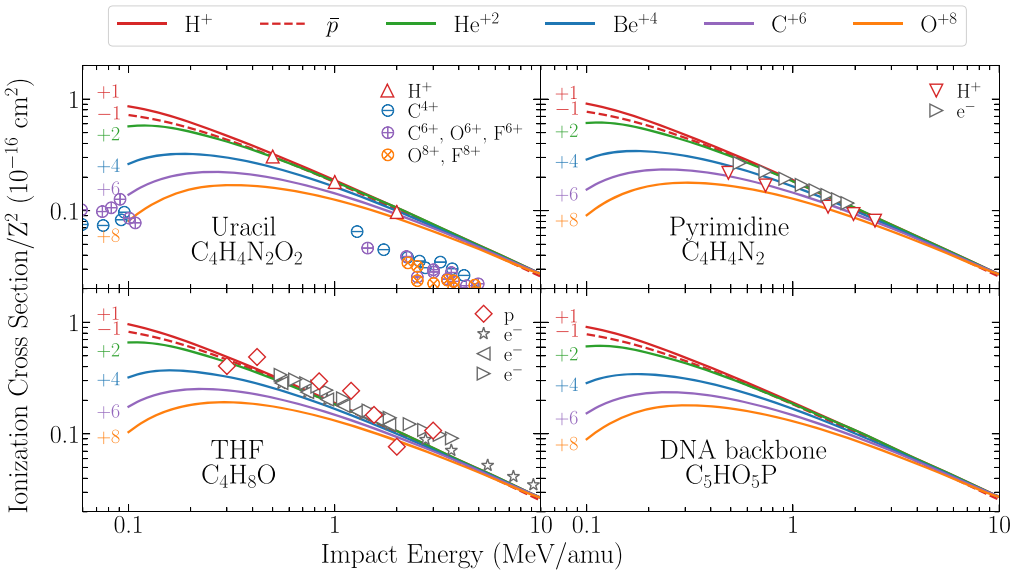

Figure 5. Reduced CDW ionization cross section σ_M/Z^2 as a function of ion impact energy. Experiments: proton impact on △ uracil [24], ▽ pyrimidine [28] and ◊ THF [29]. Impact of ⊖ C^{4+}, ⊕C^{6+}, O^{6+}, F^{6+}, and ⊗ O^{8+}, F^{8+} on uracil [25, 26]. Symbols ▷ [30], ◁ [31], and ☆ [32] for electron impact with equivelocity conversion.

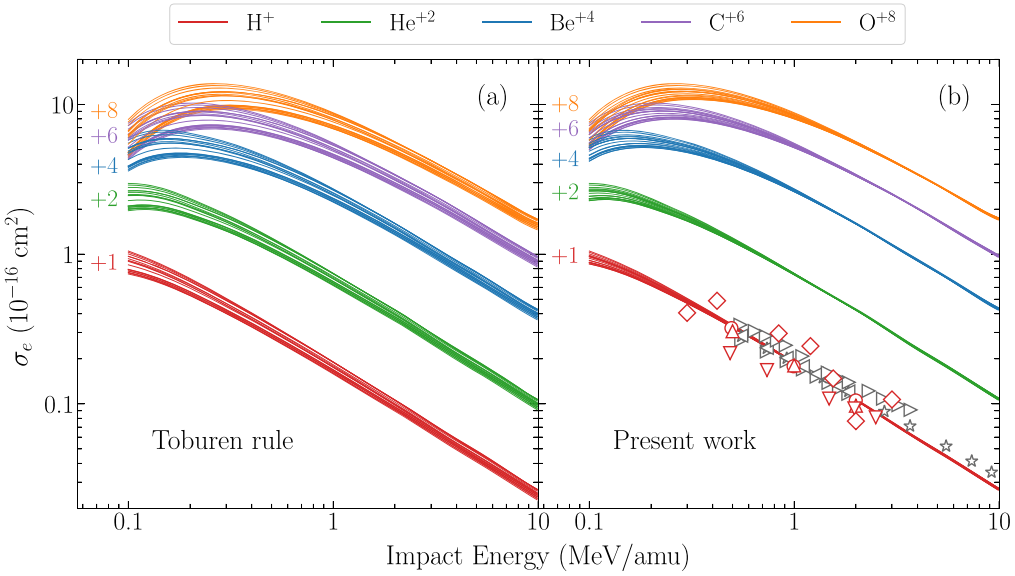

Figure 6. Scaled ionization cross section per weakly bound electron using (a) the Toburen numbers ν_α^T, and (b) our proposed numbers $\nu_\alpha^{\mathrm{CDW}}$ for molecules listed in table 1. For each band, the molecules are ordered from the smallest (top curve) to the largest (bottom curve). Experiments: proton impact on ∘ adenine [20], △ uracil [24], ▽ pyrimidine [28] and ◊ THF [29]; electron impact on ▷ pyrimidine [30], and ◁, ☆ [31, 32] THF.

or negative. This amount will depend on the relative electronegativity respect to the other atoms [42]. Following this idea, we can estimate a new number of atoms per molecule n'_α, given by

$$n'_\alpha = n_\alpha - \frac{q_\alpha}{\nu_\alpha^{\mathrm{CDW}}}. \tag{11}$$

In the case of neutral atoms, $q_\alpha = 0$ and $n'_\alpha = n_\alpha$, as it should be. In table 3, we display the average effective charge per atom q_α of C, H, N, and O, for five DNA molecules, obtained from the full molecular calculation described above.

By implementing equation (11), it is possible to determine a new stoichiometric formula (last column of table 3). Now, instead of having an integer number of atoms n_α, we obtain a fractional number n'_α. New molecular cross sections $\sigma'_M = \sum_\alpha n'_\alpha \sigma_\alpha$ can be computed considering such values. Relative errors for the ionization cross sections were computed for the DNA bases from table 3. The differences obtained were less than 3%, which indicates that the SSM is a quite robust model to handle these type of molecules within the range error expected for this model.

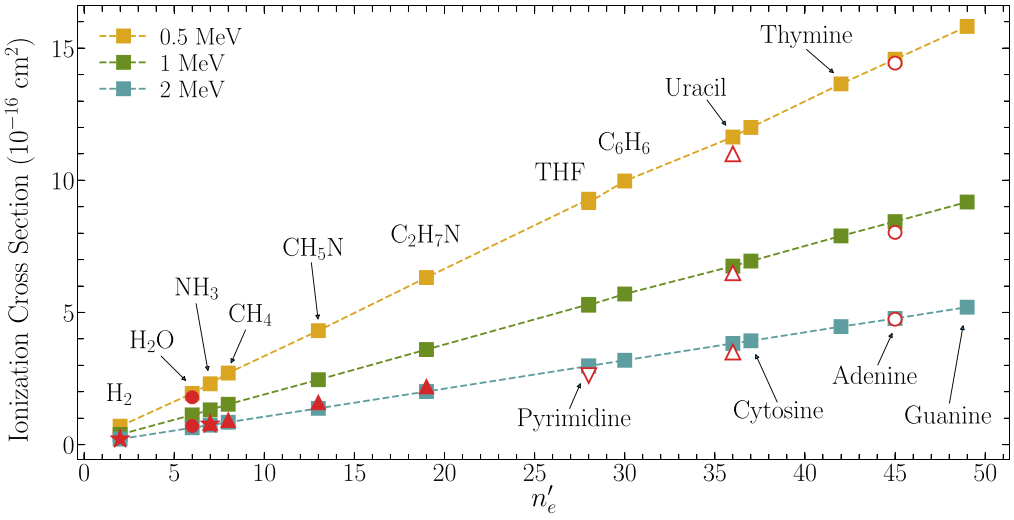

Figure 7. Ionization cross sections by the impact of protons at 0.5, 1, and 2 MeV in terms of the number of active electrons given by table 2. Experiments: ∘ adenine [20], △ uracil [24], ▽ pyrimidine [28], ▲ C_2H_7N, CH_5N, methane and ammonia [10], ⋆ ammonia and H_2 [35], and • water [36].

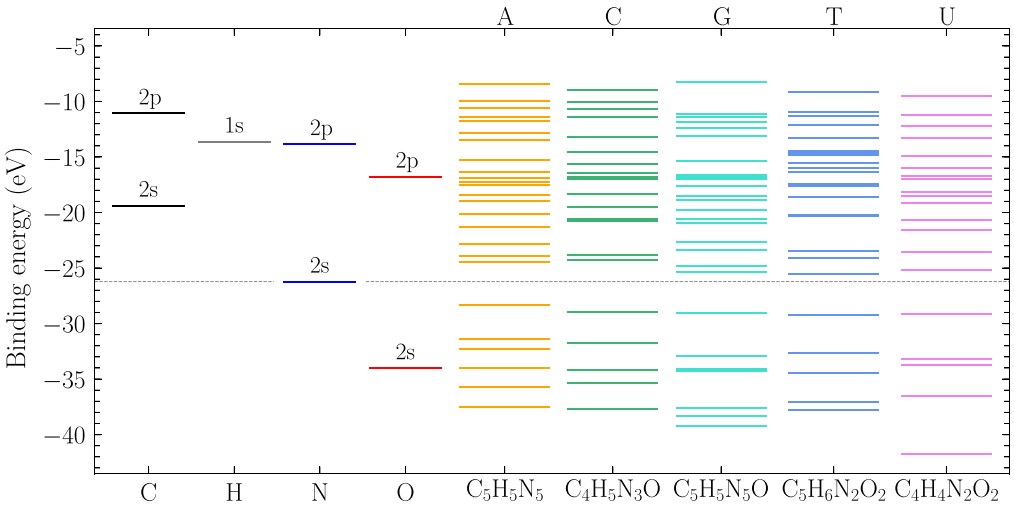

Figure 8. Theoretical molecular binding energies for adenine, cytosine, guanine, thymine, and uracil compared to those of atomic constituents.

Table 2. New scaling numbers n'_e, and Toburen numbers n_e, for some molecular targets of biological interest.

Molecule	n'_e	n_e	Molecule	n'_e	n_e	Molecule	n'_e	n_e
H_2	2	2	C_2H_7N	19	20	$C_4H_5N_3O$	37	42
H_2O	6	8	C_4H_8O	28	30	$C_5H_6N_2O_2$	42	48
NH_3	7	8	$C_4H_4N_2$	28	30	$C_5H_5N_5$	45	50
CH_4	8	8	C_6H_6	30	30	$C_5H_5N_5O$	49	56
CH_5N	13	14	$C_4H_4N_2O_2$	36	40	$C_5H_{10}O_5P$	54.5	65

4. Conclusions

In this work, we have dealt with the calculation of ionization cross sections of seventeen biological molecules containing H, C, N, O, P, and S by the impact of antiprotons, H^+, He^{2+}, Be^{4+}, C^{6+}, and O^{8+}. To that end, we have employed the full CDW method and the simple stoichiometric model. The mean energy and angle of the emitted electrons, of importance in post-collisional radiation damage, has also been calculated. Our findings show a clear dependence with the ion charge Z. For a given target as Z increases, $\overline{E}_\alpha$ also increases, but $\overline{\theta}_\alpha$ decreases, showing a clear tendency to the forward direction. At impact energies greater than 2 MeV amu^{-1}, these values converge to the Born approximation, which embodies the simple Z^2 law.

Table 3. Average effective Mulliken charge per atom q_α, and new stoichiometric formula defined by equation (11) for five DNA molecules.

Element	C	H	N	O	New stoichiometry
Adenine	+0.32	+0.23	−0.55		$C_{4.92}H_{4.77}N_{5.14}$
Cytosine	+0.28	+0.21	−0.56	−0.53	$C_{3.93}H_{4.79}N_{3.14}O_{1.13}$
Guanine	+0.46	+0.20	−0.58	−0.36	$C_{4.89}H_{4.80}N_{5.15}O_{1.09}$
Thymine	+0.20	+0.19	−0.54	−0.52	$C_{4.95}H_{5.81}N_{2.13}O_{2.13}$
Uracil	+0.31	+0.22	−0.59	−0.47	$C_{3.92}H_{3.78}N_{2.15}O_{2.12}$

Total ionization cross sections for adenine, cytosine, thymine, guanine, uracil, DNA backbone, pyrimidine, and THF are presented and compared with the scarcely available experiments. We explored the rule of Toburen, which scales all the molecular ionization cross section normalizing with a certain number of weakly bound or valence electrons. We found that the ionization cross sections scales much better when normalizing with the number of active electrons in the collision obtained from the CDW results for atoms. This new scaling was tested with good results for the six projectiles and seventeen molecules studied here. The comparison with the experimental data reinforce our findings. Furthermore, we tested the scaling by including experimental data of ionization of H_2, water, methane, and ammonia by proton impact showing good agreement at intermediate to high energies.

Finally, we performed full molecular calculations for the DNA basis. By inspecting the molecular binding energy from quantum mechanical structure calculations, we were able to understand the number of electrons proposed in our new CDW-based scaling. We attempt to improve the stoichiometric model by using the Mulliken charge to get fractional rather than integer proportions. We found no substantial correction, which indicates that the SSM works quite well.

In conclusion, the present results reinforce the reliability of the SSM to deal with complex molecules in the intermediate to high energy range. Moreover, the simple stoichiometric model and the CDW cross sections in [16] opens the possibility to describe a wide range of molecules containing H, C, N, O, P, and S, by the impact of multicharged ions.

ORCID iDs

A M P Mendez https://orcid.org/0000-0003-3568-7730

References

[1] Mohamad O, Sishc B J, Saha J, Pompos A, Rahimi A, Story M D, Davis A J and Kim D N 2017 *Cancers* **9** 66
[2] Galasssi M E, Rivarola R D, Beuve M, Olivera G H and Fainstein P D 2000 *Phys. Rev.* A **62** 022701
[3] Lüdde H J, Achenbach A, Kalkbrenner T, Jankowiak H-C and Kirchner T 2016 *Eur. Phys. J.* D **70** 82
[4] Lüdde H J, Horbatsch M and Kirchner T 2018 *Eur. Phys. J.* B **91** 99
[5] Fainstein P D, Ponce V H and Rivarola R D 1988 *J. Phys. B: At. Mol. Opt. Phys.* **21** 287
[6] Miraglia J E and Gravielle M S 2008 *Phys Rev* A **78** 052705
[7] Miraglia J E 2009 *Phys. Rev.* A **79** 022708
[8] Denifl S, Märk T D and Scheier P 2012 The role of secondary electrons in radiation damage *Radiation Damage in Biomolecular Systems* (*Biological and Medical Physics, Biomedical Engineering*) ed G García Gómez-Tejedor and M Fuss (Dordrecht: Springer)
[9] Wilson W E and Toburen L H 1975 *Phys. Rev.* A **11** 1303
[10] Lynch D J, Toburen L H and Wilson W E 1976 *J. Chem. Phys.* **64** 2616
[11] Schmidt M W *et al* 1993 *J. Comput. Chem.* **14** 1347–63
[12] Salvat F, Fernández-Varea J M and Williamson W 1995 *Comput. Phys. Commun.* **90** 151–68
[13] Mendez A M P, Mitnik D M and Miraglia J E 2016 *Int. J. Quantum Chem.* **24** 116
[14] Mendez A M P, Mitnik D M and Miraglia J E 2018 *Adv. Quantum Chem.* **76** 117–32
[15] Montanari C C and Miraglia J E 2017 *Nucl. Instrum. Meth. Phys. Res.* B **407** 236–43
[16] Miraglia J E 2019 (arXiv:1909.13682 [physics.atom-ph])
[17] Surdutovich E and Solov'yov A V 2013*AIP Conference Proceedings* **1525** 672
[18] de Vera P, Abril I, Garcia-Molina R and Solov'yov A V 2013 *J. Phys.: Conf. Ser.* **438** 012015
[19] Rudd M E, Kim Y-K, Madison D H and Gay T J 1992 *Rev. Mod. Phys.* **64** 441–90
[20] Iriki Y, Kikuchi Y, Imai M and Itoh A 2011 *Phys. Rev.* A **84** 052719
[21] Rahman M A and Krishnakumar E 2016 Electron ionization of DNA bases *J. Chem. Phys.* **144** 161102
[22] Mozejko P and Sanche L 2003 *Radiat. Environ. Biophys.* **42** 201
[23] Tan H Q, Mi Z and Bettiol A A 2018 *Phys. Rev.* E **97** 032403
[24] Itoh A, Iriki Y, Imai M, Champion C and Rivarola R D 2013 *Phys. Rev.* A **88** 052711
[25] Agnihotri A N *et al* 2012 *Phys. Rev.* A **85** 032711
[26] Agnihotri A N *et al* 2013 *J. Phys. B: At. Mol. Opt. Phys.* **46** 185201
[27] Champion C, Galassi M E, Fojón O, Lekadir H, Hanssen J, Rivarola R D, Weck P F, Agnihotri A N, Nandi S and Tribedi L C 2012 *J. Phys.: Conf. Ser.* **373** 012004
[28] Wolff W, Luna H, Sigaud L, Tavares A C and Montenegro E C 2014 *J. Chem. Phys.* **140** 064309
[29] Wang M, Rudek B, Bennett D, de Vera P, Bug M, Buhr T, Baek W Y, Hilgers G and Rabus H 2016 *Phys. Rev.* A **93** 052711
[30] Bug M U, Baek W Y, Rabus H, Villagrasa C, Meylan S and Rosenfeld A B 2017 *Radiat. Phys. Chem.* **130** 459–79
[31] Wolff W, Rudek B, da Silva L A, Hilgers G, Montenegro E C and Homem M G P 2019 *J. Chem. Phys.* **151** 064304
[32] Fuss M, Muñoz A, Oller J C, Blanco F, Almeida D, Limão-Vieira P, Do T P D, Brunger M J and García G 2009 *Phys. Rev.* A **80** 052709
[33] Janev R K and Presnyakov L P 1980 *J. Phys. B: At. Mol. Phys.* **13** 4233
[34] DuBois R D, Montenegro E C and Sigaud G M 2013 *AIP Conf. Proc.* **1525** 679
[35] Rudd M E, Kim Y-K, Madison D H and Gallagher J W 1985 *Rev. Mod. Phys.* **57** 965–94

[36] Luna H *et al* 2007 *Phys. Rev.* A **75** 042711
[37] Lüdde H J, Horbatsch M and Kirchner T 2019 *J. Phys. B: At. Mol. Opt. Phys.* **52** 195203
[38] Hush N S and Cheung A S 1975 *Chem. Phys. Lett.* **34** 11
[39] Verkin B I, Sukodub L F and Yanson I K 1976 *Dokl. Akad. Nauk SSSR* **228** 1452
[40] Dougherty D, Younathan E S, Voll R, Abdulnur S and McGlynn S P 1978 *J. Electron Spectrosc. Relat. Phenom.* **13** 379
[41] Lee J-G, Jeong H Y and Lee H 2003 *Charges Bull. Korean Chem. Soc.* **24** 369
[42] Rappe A K and Goddard W A III 1991 *J. Phys. Chem.* **95** 3358